Supplementary Information for:

Floods on a Schedule: Coastal Flooding at Consistent Hours

Joris G. W. Beemster[1,*], Stefan A. Talke[2], Ivan D. Haigh[3,4], Ben S. Hague[5,6], Grace C. Levins[6], Dirk S. van Maren[7,8], and Antonius J. F. Hoitink[1]

[1]Department of Environmental Sciences, Wageningen University & Research, Droevendaalsesteeg, Wageningen, 6708 PB, The Netherlands
[2]Department of Civil and Environmental Engineering, California Polytechnic State University, Grand Ave, San Luis Obispo, 93407, California, USA
[3]School of Ocean and Earth Science, University of Southampton, European Way, Southampton, SO14 3ZH, Hampshire, UK
[4]National Centre for Integrated Coastal Research and Dept. of Civil, Environmental and Construction Engineering, University of Central Florida, Pegasus Drive, Orlando, 32816, Florida, The United States of America
[5]Australian Bureau of Meteorology, Collins St, Docklands, 3087, Victoria, Australia
[5]School of Earth, Atmosphere and Environment, Monash University, Clayton, Victoria, Australia
[7]Marine and Coastal Systems, Deltares, Boussinesqweg, Delft, 2629 HV, The Netherlands
[8]Faculty of Civil Engineering and Geosciences, Delft University of Technology, Mekelweg, Delft, 2628 CD, The Netherlands

[*]Correspondence: `joris.beemster@wur.nl`

This PDF file includes:

- Supplementary Notes 1-2
- Supplementary Tables 1-2
- Supplementary Figures 1–3
- Supplementary References

Supplementary Note 1 | Phase-wrapping of tidal constituents with the solar day or year

When the phases of two tidal constituents drift relative to a solar day or year, their superposition can produce distinct *phase-wrapping* patterns, periodic modulations of amplitude and phase that repeat on solar-day or solar-year timescales. These modulations explain why the time of high water, or the number of distinct peaks per solar day, can vary systematically through the fortnightly, annual, or semiannual cycles.

Any constituent i can be expressed as

$$\zeta_i(t) = A_i \cos(2\pi f_i t + \phi_i),$$

where f_i is the frequency in cycles per solar day. This frequency can be decomposed as

$$f_i = k_i + \delta_i,$$

where k_i is an integer species number (0 = long-period, 1 = diurnal, 2 = semidiurnal, etc.) and δ_i is a small alias offset that causes the phase to drift relative to the solar day. To address solar year wrapping, one can adjust this relationship to units of cycles per solar year (f_i becomes F_i). When $\delta_i = 0$, as for S_1 and S_2, the constituent is locked to the solar day and produces recurring times of day with elevated water levels.

In addition to single constituents, pairs of constituents (i, j) can phase-lock with the solar-day if the ratio R of their alias offsets (δ_i, δ_j) is a rational number p/q:

$$R = \frac{\delta_i}{\delta_j} = \frac{p}{q}, \qquad p, q \in \mathbb{Z} \text{ in lowest terms.}$$

When this condition is met, their combined signal produces a repeating pattern within the reference frame (solar day or solar year). Pairs of constituents that are exact harmonics of one another (e.g., $M_4 = 2M_2$) do not generate cyclic modulation patterns in the solar reference frame, as their phases remain locked through harmonic dependence rather than solar aliasing. Such pairs are therefore excluded. The number of distinct peaks (or bands) that appear when the tidal time series is folded over the solar day or year is

$$N_{\text{peaks}} = |k_i q - k_j p|.$$

The aliasing period of the constituent pair relative to the solar day is

$$T_{\text{alias}} = \frac{1}{|\delta_i - \delta_j|}.$$

If T_{alias} is shorter than the wrapping period (solar day or year), the wrapping pattern will already appear within a single cycle of that period. If T_{alias} exceeds the wrapping period, the

time required to fully populate the wrapped window is given by

$$T_{\text{repeat}} = \left|\frac{p}{\delta_i}\right| = \left|\frac{q}{\delta_j}\right|.$$

The same framework applies to any pair of tidal constituents and provides a unified way to predict when phase-wrapping will occur, how many peaks emerge in the solar frame, and over what interval the pattern repeats. Tables 1 and 2 summarize the constituent (pairs) at Boston that phase-lock with the solar day and year, with expected amplitudes exceeding 1 cm.

Example 1 – Diurnal wrapping ($\mathbf{P_1}$–$\mathbf{K_2}$)

For the diurnal–semidiurnal pair P_1 ($f = 0.99726$ cpd) and K_2 ($f = 2.00548$ cpd), the alias offsets are $\delta_{P1} = -0.00274$ and $\delta_{K2} = 0.00548$ cpd, giving $R = p/q = -1/2$). When folded over the solar day, the two constituents yield

$$N_{\text{peaks}} = |k_i q - k_j p| = |1 \cdot 2 - 2 \cdot (-1)| = 4$$

preferred high-water times per day. The aliasing period is $T_{\text{alias}} = 121$ days, which exceeds the solar-day wrapping period. Consequently, the time for the full pattern to repeat is exactly a solar year:

$$T_{\text{repeat}} = \left|\frac{p}{\delta_i}\right| = \left|\frac{q}{\delta_j}\right| = \left|\frac{1}{-0.00274}\right| = \left|\frac{2}{0.00548}\right| = 365.24 \text{ days}.$$

Example 2 – Annual wrapping ($\mathbf{P_1}$–$\mathbf{K_2}$)

For the same pair, we can express the frequencies in cycles per solar year: $F_{P1} = 364.2425$ cpy and $F_{K2} = 732.4851$ cpy. The corresponding alias offsets are $\Delta_{P1} = 0.2425$ and $\Delta_{K2} = 0.4851$ cpy, giving $R = p/q = 1/2$). When folded over the solar year, the combined tide yields

$$N_{\text{peaks}} = |k_i q - k_j p| = |364 \cdot 2 - 732 \cdot 1| = 4$$

preferred high-water times per year. Here, the aliasing period $T_{\text{alias}} = 121$ days is shorter than the wrapping period (1 year), meaning that the full pattern appears within each solar year. Thus, the effective wrapping period is one year, during which the four peaks fill the solar-year frame.

The same framework applies to any pair of tidal constituents and provides a unified way to predict when phase-wrapping will occur, how many peaks emerge in the solar frame, and over what interval the pattern repeats.

Supplementary Note 2 | Sea-level rise

Sea-level rise (SLR) is expected to fundamentally alter not only the frequency but also the timing of coastal flood events. Using San Diego, California, as a case study (Figure 3), we examine how the hourly distribution of flood threshold exceedances evolves under (NOAA) Low, Intermediate, and High SLR scenarios [1].

Initially, exceedances emerge at the same peak flood hours identified under present-day conditions. However, as sea level continues to rise, these exceedances gradually spread to all hours of the day, shifting from a temporally predictable flooding hazard to a state of near-permanent flooding. The rate of this spread is strongly dependent on the SLR scenario. Under Low SLR, the transition from clustered to continuous exceedances can take more than a century. In contrast, under Intermediate and High SLR, this transition occurs much more rapidly, eventually leading to daily flooding with no preferred timing.

A key inflection point occurs when mean higher high water (MHHW) surpasses the current flood thresholds. At this stage, flooding becomes a baseline condition and exceedances are no longer tied to specific lunar phases. Prior to this, we observe a shift in the impact severity of clustered events: What are currently classified as minor floods begin to reach moderate or major thresholds, while still occurring around the original tidal modes.

Supplementary Tables

Table 1. Tidal constituent interactions within the solar day at Boston (8443970). Largest tidal constituent pairs (where the amplitude of the smaller constituent ≥ 0.01 m) leading to clustering within the solar day. *N Peaks* denotes the number of clustering peaks within the solar day, and *Amplitude* represents the amplitude of the smaller constituent in the pair, providing an indication of the relative importance of the constituent interaction. *Repeat time* indicates the duration required for the phase-wrapped pattern to fully repeat.

Constituent pair	**N Peaks**	**Amplitude (m)**	**Repeat time (days)**
S_2	2	0.208	1
Sa - K_1	1	0.049	365.24
Sa - K_2	2	0.049	365.24
Sa - P_1	1	0.047	365.24
P_1 - K_1	2	0.047	365.24
P_1 - K_2	4	0.047	365.24
Ssa - K_2	2	0.022	182.62
Ssa - K_1	2	0.022	365.24
Ssa - P_1	2	0.022	365.24
Sa - T_2	2	0.018	365.24
Ssa - T_2	4	0.018	365.24
P_1 - T_2	1	0.018	365.24
K_1 - T_2	3	0.018	365.24
K_2 - T_2	6	0.018	365.24
μ_2 - M_2	2	0.010	14.77
μ_2 - M_4	2	0.010	7.38
μ_2 - M_6	6	0.010	14.77

Table 2. Tidal constituent interactions within the solar year at Boston (8443970). Largest tidal constituent pairs (where the amplitude of the smaller constituent ≥ 0.01 m) leading to clustering within the solar year. *N Peaks* denotes the number of clustering peaks within the solar year, and *Amplitude* represents the amplitude of the smaller constituent in the pair, providing an indication of the relative importance of the constituent interaction. *Repeat time* indicates the duration required for the phase-wrapped pattern to fully repeat.

Constituent pair	**N Peaks**	**Amplitude (m)**	**Repeat time (days)**
S_2 - K_1	2	0.143	365.24
S_2 - K_2	2	0.059	365.24
Sa	1	0.049	365.24
P_1 - K_1	2	0.047	365.24
P_1 - S_2	2	0.047	365.24
P_1 - K_2	4	0.047	365.24
Ssa	2	0.022	365.24
P_1 - T_2	1	0.018	365.24
K_1 - T_2	3	0.018	365.24
T_2 - S_2	1	0.018	365.24
T_2 - K_2	3	0.018	365.24

Supplementary Figures

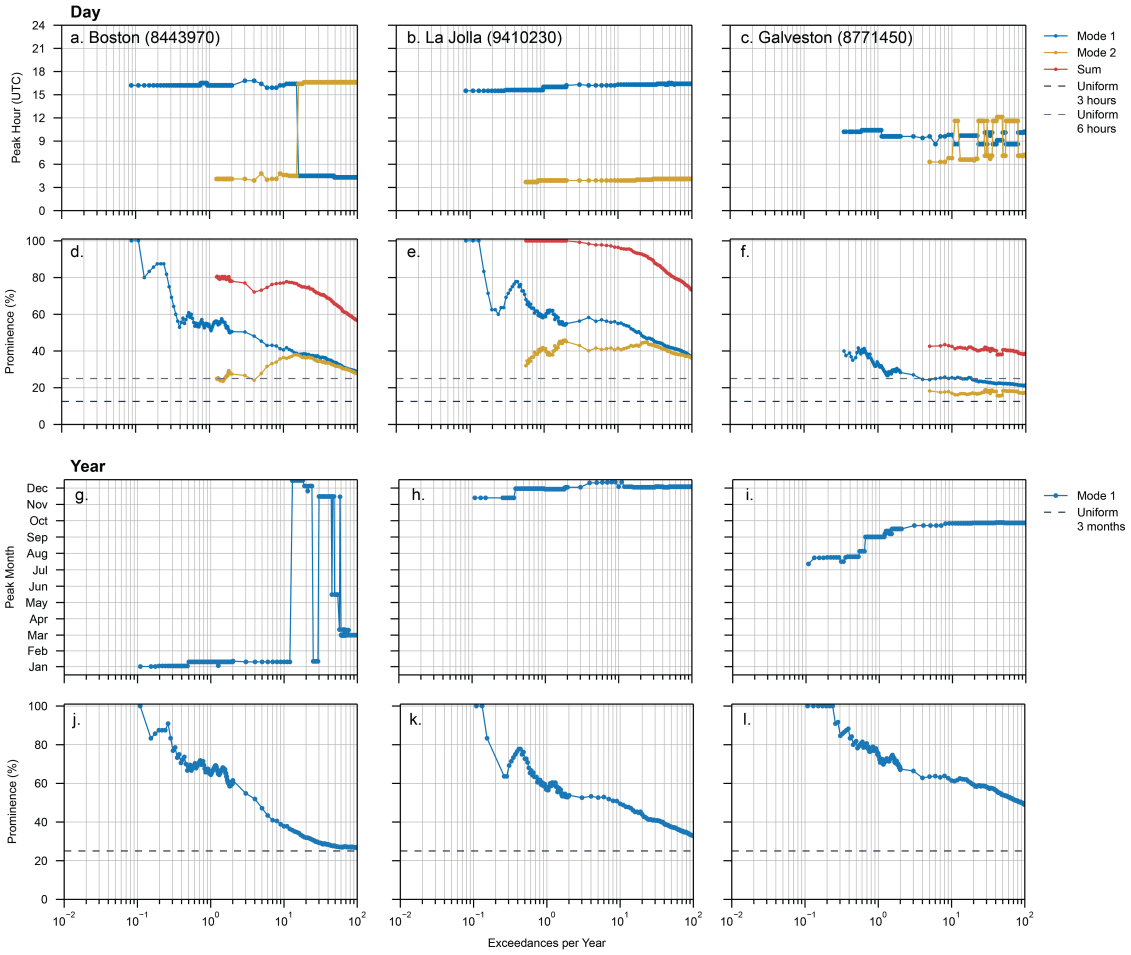

Figure 1. Intraday and intrayear clustering characteristics of tidal peak timings across three U.S. tide gauge stations. (a–c) Times of occurrence for Mode 1 and Mode 2 of intraday clustering, shown for different recurrence intervals at Boston, La Jolla, and Galveston. (d–f) Prominence of Mode 1, Mode 2, and their combined contribution, expressed as the percentage of peaks within each mode relative to the total number of peaks. (g–i) Times of occurrence for the dominant intrayear mode at the same stations. (j–l) Corresponding prominence of the intrayear mode. Only statistically significant values are shown ($p < 0.01$).

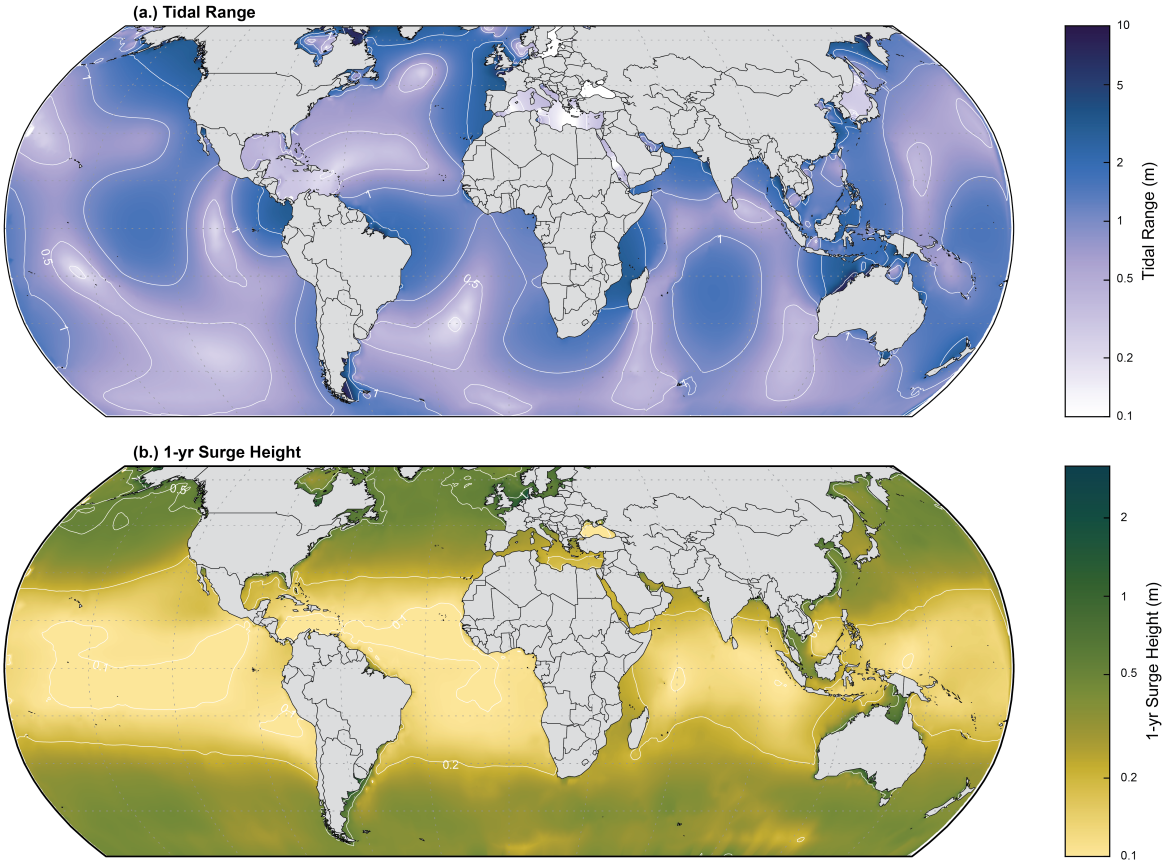

Figure 2. Global distribution of tidal range and 1-year recurrence surge height from the Global Tide and Surge Model (GTSM)[2, 3]. (a) Tidal range (mean high water minus mean low water). (b) 1-year recurrence surge height. Both maps use a logarithmic color scale to highlight spatial variability across several orders of magnitude. Data are interpolated from 43,119 GTSM output locations. High-latitude regions near the poles are excluded due to expected limitations in model performance.

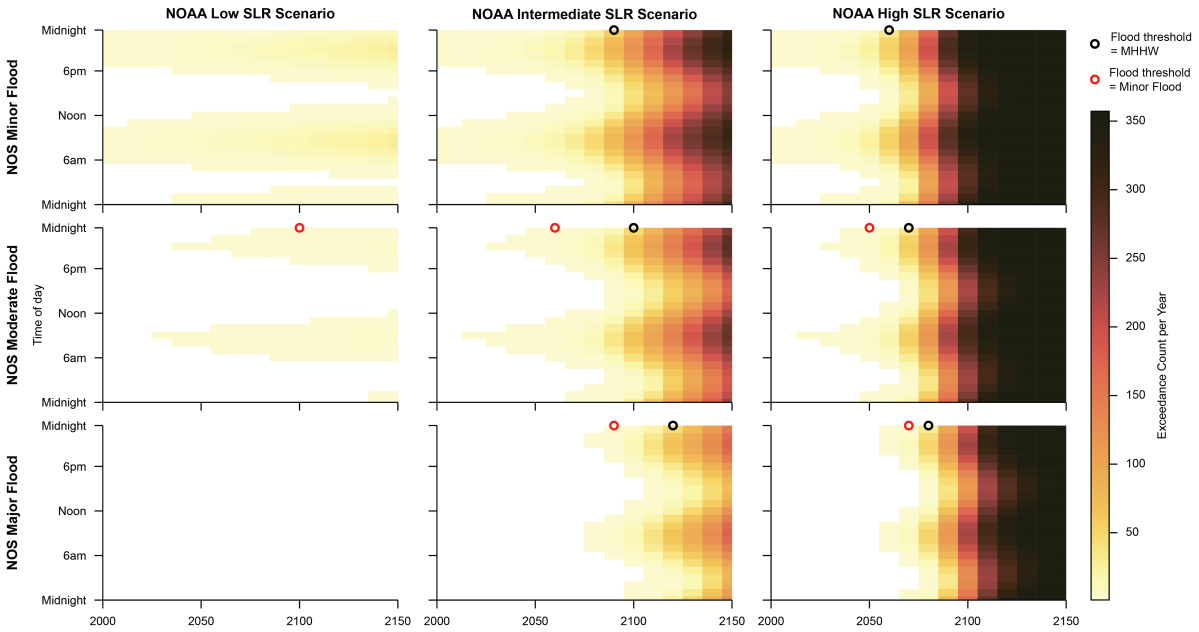

Figure 3. Projected shifts in flood timing under sea-level rise scenarios for San Diego: Hourly distribution of flood threshold exceedances per year at San Diego (NOAA ID: 9410170) under three NOAA sea-level rise (SLR) scenarios: Low, Intermediate, and High (columns). Rows correspond to NOAA NOS flood thresholds: Minor (top), Moderate (middle), and Major (bottom) [1]. Color shading indicates the number of exceedances per hour per year. Black markers denote the year when the present-day threshold aligns with the projected Mean Higher High Water (MHHW), indicating a shift in baseline conditions. Red markers indicate when today's moderate or major flood levels become equivalent to future minor flood thresholds.

Supplementary References

References

[1] Sweet, W. V. *et al.* Global and Regional Sea Level Rise Scenarios for the United States: Updated Mean Projections and Extreme Weather Level Probabilities along US Coastlines (2022).

[2] Muis, S. *et al.* A high-resolution global dataset of extreme sea levels, tides, and storm surges, including future projections. *Front. Mar. Sci.* **7**, 263 (2022).

[3] Muis, S. *et al.* Global projections of storm surges using high-resolution CMIP6 climate models *Earth's Future* **11** e2023EF003479 (2023).